

### III. 研究成果の刊行に関する一覧表

研究成果の刊行に関する一覧表

書籍

著者氏名	論文タイトル名	書籍全体の編集者名	書籍名	出版社名	出版地	出版年	ページ
井上幸次	ヒトヘルペスウイルス感染症,	村田敏規	専門医のための眼科診療クオリファイ5 全身疾患と眼	中山書店	東京	2011	124-128

雑誌

発表者氏名	論文タイトル名	発表誌名	巻号	ページ	出版年
Zheng X, Shiraishi A, Okuma S, Mizoue S, Goto T, Kawasaki S, Uno T, Miyoshi T, Ruggeri A, <u>Ohashi Y</u>	In vivo confocal microscopic evidence of keratopathy in patients with pseudoexfoliation syndrome.	Invest Ophthalmol Vis Sci	52(3)	1755-1761	2011
Zheng X, Sakai H, Goto T, Namiguchi K, Mizoue S, Shiraishi A, Sawaguchi S, <u>Ohashi Y</u>	Anterior segment optical coherence tomography analysis of clinically unilateral pseudoexfoliation syndrome: evidence of bilateral involvement and morphological factors related to asymmetry.	Invest Ophthalmol Vis Sci	52(8)	5679-5684	2011
Hatou S, Shimmura S, Shimazaki J, Usui T, Amano S, Yokogawa H, Kobayashi A, Zheng X, Shiraishi A, <u>Ohashi Y</u> , Inatomi T, Tsubota K	Mathematical projection model of visual loss due to fuchs corneal dystrophy.	Invest Ophthalmol Vis Sci	52(11)	7888-7893	2011
Miyazaki D, Haruki T, Takeda S, Sasaki S, Yakura K, Terasaka Y, Komatsu N, Yamagami S, Touge H, Touge C, <u>Inoue Y</u>	Herpes simplex virus type 1-induced transcriptional networks of corneal endothelial cells indicate antigen presentation function.	Invest Ophthalmol Vis Sci	52(7)	4282-4293	2011
Takeda S, Miyazaki D, Sasaki S, Yamamoto Y, Terasaka Y, Yakura K, Yamagami S, Ebihara N, <u>Inoue Y</u>	Roles played by toll-like receter-9 in corneal endothelial cells after herpes simplex virus type 1 infection.	Invest Ophthalmol Vis Sci	52(9)	6729-6736	2011

井上幸次	全身疾患に関連したヒトヘルペスウイルス眼感染症	鳥取医学雑誌	39	1-5	2011
小泉範子	眼感染アレルギーセミナー— 感染症と生体防御— 30. サイト トメガロウイルス角膜内皮炎	あたらしい眼科	28(10)	1439-1440	2011

#### IV. 研究成果の刊行物・別刷

## ヒトヘルペスウイルス感染症

### 種類

ヒトヘルペスウイルス (human herpes virus ; HHV) は現在 8 種が知られており,  $\alpha$ ,  $\beta$ ,  $\gamma$  の三つの亜科に分けられている (表 1). ヘルペスウイルスは人体に潜伏感染をする性質やヒトの免疫を巧みに回避するさまざまな仕組みをもっている. そのことによって, ヒトに寄生しながら人類とともに歩んできたウイルスであり, 全身のさまざまな臓器に多岐にわたる感染症を引き起こしてくる. 一方, 眼においても  $\alpha$  ヘルペスウイルスは特に眼感染症の原因ウイルスとして古くから知られており,  $\beta$  ヘルペスウイルスも重要な眼感染症の原因ウイルスとして最近話題になっている. また,  $\gamma$  ヘルペスウイルスも眼との関連がいわれている.

本項では, ヒトヘルペスウイルス感染症で, 全身疾患との関連で論じることのできるものを中心にまとめた.

### 単純ヘルペスウイルス

単純ヘルペスウイルス (herpes simplex virus ; HSV) は神経向性があり, 神経節に潜伏感染する特徴がある. 年齢が進むとともに潜伏感染率は上昇していくが, 最近わが国では, 若年者における未感染者が増加している. HSV は多彩な感染症を引き起こすが, 1 型と 2 型があり (HSV-1, HSV-2), 顔面の皮疹や口唇ヘルペスは HSV-1 によるものが多く, 特にヘルペス性角膜炎はほとんど HSV-1 による. 一方, 性器ヘルペスは HSV-2 によるものが多い. HSV は潜伏と再発を繰り返して宿主を悩ますが, 宿主を殺すことは滅多にない. しかし, まれに重篤なヘルペス脳炎で死亡するケースもある.

HSV による眼感染症 (眼瞼単純疱疹, ヘルペス性結膜炎, ヘルペス性角膜炎, 急性網膜壊死) を起こす患者の多くは, ほかに全身疾患をもたない免疫正常者である. HSV による眼感染症と性器ヘルペスを同時に起こすようなことはなく, ましてヘルペス脳炎を発症するようなこともない. そういう点で, HSV はヘルペスウイルスのな

表1 ヒトヘルペスウイルスの種類

系統名	一般名	和名	亜科
HHV-1	herpes simplex virus type 1	単純ヘルペスウイルス1型	$\alpha$
HHV-2	herpes simplex virus type 2	単純ヘルペスウイルス2型	$\alpha$
HHV-3	varicella-zoster virus	水痘帯状疱疹ウイルス	$\alpha$
HHV-4	human cytomegalovirus	ヒトサイトメガロウイルス	$\beta$
HHV-5	Epstein-Barr virus	エプスタイン-バーウイルス	$\gamma$
HHV-6	human herpes virus-6	ヒトヘルペスウイルス6	$\beta$
HHV-7	human herpes virus-7	ヒトヘルペスウイルス7	$\beta$
HHV-8	Kaposi's sarcoma-associated herpesvirus	ヒトヘルペスウイルス8 (カポジ肉腫関連ヘルペスウイルス)	$\gamma$

HHV : human herpes virus

かで最も眼感染症の頻度が高いにもかかわらず、全身疾患との関連はあまりないといえる。ただ、例外として、アトピー性皮膚炎 (atopic dermatitis ; AD) と関連した HSV 眼感染症が問題となる。

アトピー性皮膚炎との関連：AD はアレルギー反応によって、痒痒感の強い特徴的な慢性皮膚炎症の寛解と増悪を繰り返す疾患である。遺伝的素因と環境因子の両者がこの疾患の発症と関与しているが、わが国では最近 AD 患者が非常に増加し、世界でも有数の罹病率となっている。AD ではアトピー性角結膜炎・アトピー白内障・円錐角膜・網膜剥離など、多くの眼合併症を併発してくることが知られているが、感染症を起こしやすいことも問題である。特に黄色ブドウ球菌と HSV が問題となる。

AD には重症のヘルペス皮膚感染を生じることがあり、カポジ水痘様発疹 (Kaposi's varicelliform eruption ; KVE)<sup>\*1</sup> となる。その機序については不明な点も多いが、最も大きな要因としては、HSV に対する細胞性免疫の不全が考えられている<sup>1)</sup>。また、正常皮膚に比較して AD 患者の皮膚では HSV が増殖しやすいこと<sup>2)</sup>、手で掻くことが皮膚での HSV 感染を広げる要因となっていること<sup>3)</sup> なども報告されている。

KVE では眼表面にも HSV の感染が及ぶ可能性が高く、ヘルペス性角膜炎が KVE に合併してくることがある。また、KVE が顔面片側に限局している場合に帯状疱疹様にみえることがあり、帯状単純疱疹 (zosteriform simplex) といわれている。

アトピー性皮膚炎患者でのヘルペス性角膜炎の特徴：AD 患者は前

**[\*1]** カポジ水痘様発疹 eczema herpeticum (EH) ともいわれており、1887年に Kaposi によって最初に報告された。湿疹様皮膚に HSV が感染することによって生じる広範な水疱性疾患であり、皮膚症状のみならず、発熱、倦怠感、所属リンパ節腫脹を伴うこともある。このカポジ水痘様発疹の基礎疾患としてアトピー性皮膚炎が最も多く、また重要である。

文献は p.274 参照。

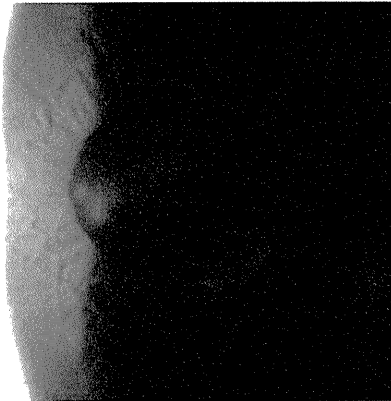


図1 アトピー性皮膚炎患者に生じた樹枝状癢痕 (37歳, 男性)

何度も上皮型ヘルペスを生じ, 樹枝状の上皮下混濁が残存している。

記のように皮膚にHSV感染を生じている場合のみならず, 一般に角膜においてもヘルペスを起こしやすいことが知られている。AD患者におけるヘルペス性角膜炎は両眼性が多く (ただし同時発症はまれ), 主として上皮型であり, 再発が多く, また上皮の修復が遅いために表層実質に癢痕が残りやすいことが報告されている (図1)<sup>4)</sup>。また, AD患者ではアシクロビル耐性株による角膜ヘルペスの発症が報告されている<sup>5)</sup>。もともとアシクロビル耐性株は増殖力が弱いことが多いが, AD患者ではこのように増殖しにくいウイルスにも病気を生じさせる力を与えてしまうことになる。

### 水痘帯状疱疹ウイルス

眼科領域では帯状ヘルペスウイルスと呼称される場合があるが, 水痘帯状疱疹ウイルス (varicella-zoster virus; VZV) が正式な名称である。

名前のとおり, VZVの初感染は水痘の形で生じる。VZVは最初上気道に感染し, ウイルス血症を生じた後に, 全身に水疱を生じ, やがて終息する。しかしHSV同様に神経向性があり, 各神経節に潜伏感染が成立する。これが年余を経て再活性化したものが帯状疱疹である。そして, 三叉神経第1枝領域に生じると眼部帯状疱疹としてさまざまな眼合併症を生じてくる。

VZVはHSVと異なり, 再発病変としての帯状疱疹を生じるのは生涯に一度のことがほとんどである。しかし, 単純疱疹と異なり, その範囲は広く, 神経痛を含めて合併症も多彩で重症となる。

**眼部帯状疱疹 (herpes zoster ophthalmicus):** VZVによる眼合併症は多彩であり, 結膜炎, 上皮型角膜炎<sup>\*2)</sup>, 実質型角膜炎<sup>\*3)</sup>, 上強膜炎, 強膜炎, 虹彩炎<sup>\*4)</sup>, 虹彩萎縮, 眼筋麻痺, 涙腺炎など, きわ

**\*2) 上皮型角膜炎**  
VZVによる上皮型は, terminal bulbを認めない細く小さい偽樹枝状角膜炎や星状角膜炎を呈する。

**\*3) 実質型角膜炎**  
VZVによる実質型は, 小溷潤から銭型, 円板状など種々の大きさを呈し, 部位も中央, 周辺を含めさまざまである。

**\*4) 虹彩炎**  
VZVによる虹彩炎は, 豚脂様角膜後面沈着物を伴う肉芽腫性を呈する。

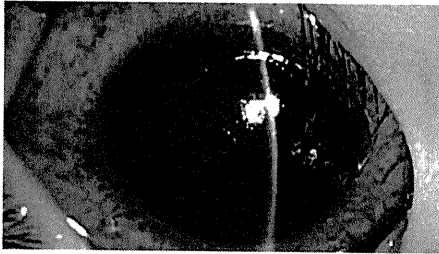


図2 水痘角膜炎

(1歳4か月, 女児)

角膜実質浅層中心の斑状混濁と上方よりの血管侵入, 強い毛様充血と結膜充血を認める.

(写真提供: 鳥取市立病院 細川満人先生.)

めて多彩である。眼部带状疱疹の眼合併症は、活発なウイルス増殖よりも免疫反応を反映したものとなり、治療にステロイドを十分に使用することが推奨されている。いったん終息すればHSVの場合と異なり再発することはきわめてまれだが、遷延例はかなり認められ、また、ステロイド点眼で消炎した際に早期にやめると、再燃することがある。眼合併症は皮疹のピークよりも遅れて生じてくることが多いので、初診で眼所見がなくても引き続き経過観察が必要である。その際、Hutchinsonの法則<sup>\*5</sup>は診療上役に立つ。

**水痘角膜炎 (varicella keratitis) :** 水痘罹患後数か月を経て、片眼に円板状角膜炎の形で、角膜中央の浮腫と混濁を生じてくることがまれにあり、水痘角膜炎といわれている(図2)。小児において、水痘罹患後まもなく、その続発症として生じる。直接の角膜への感染による病態か、一度潜伏したVSVの再活性化による病態であるかは不明である。ステロイド点眼とアシクロビル眼軟膏で軽快するが、早期にやめると再燃することが多く、弱視の発症も伴うため、健眼と同等の良好な視力を得ることが難しい。

**進行性網膜外層壊死 (progressive outer retinal necrosis ; PORN) :** 急性網膜壊死は免疫正常者の網膜内層に発症し、病態にウイルス増殖と免疫反応による炎症の両方が関与しており、炎症が強くと、前眼部炎症や硝子体混濁も伴うが、このPORNは免疫不全の患者の網膜の外層に急激に発症・拡大する。視力予後はきわめて不良である。

### ヒトサイトメガロウイルス

human cytomegalovirus (HCMV) によるサイトメガロウイルス網膜炎は、免疫不全の患者に起こるのが大きな特徴である。それ以外の臓器でもHCMVは免疫不全に伴って感染を起こしてくる。ただ、最近話題となっているサイトメガロウイルス虹彩炎、角膜内皮炎はその例外といえる。

**臨床的特徴 :** サイトメガロウイルス網膜炎は免疫不全の患者に、多

#### **[\*5] Hutchinsonの法則**

带状疱疹で、鼻尖・鼻翼に皮疹があれば眼合併症を起こしてくる頻度が高い、という法則。これは、鼻と眼がどちらも三叉神経第1枝の枝である鼻毛様体神経の支配を受けていることによる。

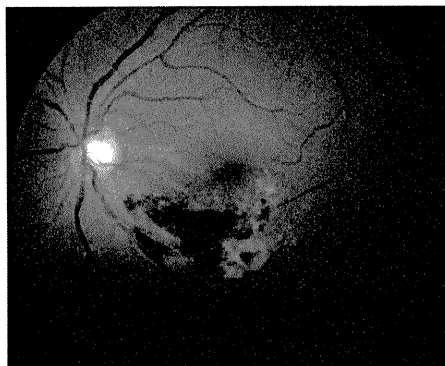


図3 サイトメガロウイルス網膜炎 (29歳, 女性)  
後極部血管を中心とした出血・滲出斑を認める。

くは両眼性に起こる。AIDSの重要な症状の一つであったが、それに関しては、近年 highly active anti-retroviral therapy (HAART)<sup>\*6</sup>の導入により、その頻度は減少している。臨床所見としては後極部の血管周囲の出血・滲出斑を特徴としている(図3)。免疫不全で生じるため、硝子体混濁や前眼部炎症は認められないか、あってもごく軽度である。

**検査:** 眼局所においてはPCRによる前房や硝子体からのウイルスDNA検出が重要であるが、CMVで網膜炎を起こしている患者の場合、免疫不全を背景として全身の他の臓器の感染の可能性もあり、血清の抗CMV抗体価の上昇、血清のCMV抗原血症(antigenemia)の証明などの全身的なウイルス検索も重要となる。

**治療:** 抗CMV薬(ガンシクロビル, バルガンシクロビル)の投与とともに、免疫不全の改善が必要だが、改善に伴い炎症が生じることもあるので注意が必要である(immune recovery uveitis<sup>\*7</sup>)。

### その他のヘルペスウイルス

その他のヘルペスウイルス属についても眼感染症の原因ウイルスとしての報告があるが、確立されたものは少ない。Epstein-Barr virus (HHV-5) や HHV-6 は HCMV とともに造血幹細胞移植後に再活性化をすることが報告されており、免疫不全患者でのさまざまな合併症に関連している可能性が指摘されているが、そのような場合において眼感染症に関与したという報告はまだない。

HHV-8 は AIDS 患者のカポジ肉腫から発見されたウイルスであり、当然眼瞼のカポジ肉腫の原因ウイルスである。これは AIDS などの免疫不全患者で生じるので、その他のヘルペスウイルスに関して全身疾患と関連した唯一確かなものであるといえる。

(井上幸次)

#### ※6 HAART

抗 HIV 治療において、非核酸系逆転写酵素阻害薬、プロテアーゼ阻害薬のいずれかと核酸系逆転写酵素阻害薬 2 剤を含む 3 剤以上の抗ウイルス薬を組み合わせる強力な多剤併用療法のこと。この導入により、AIDS は罹患者が死亡する病気から生存可能な病気となった。

#### ※7 immune recovery uveitis

HAART などの導入により、CMV 網膜炎を有する患者で臨床的な免疫能の回復に伴って眼内炎症を生じるケースが認められるようになり、こう呼ばれている。強い前房内や硝子体の炎症を生じてくればステロイドによる治療が必要となり、硝子体混濁、黄斑浮腫、網膜上膜などを合併してくれば硝子体手術が必要となることもある。

# In Vivo Confocal Microscopic Evidence of Keratopathy in Patients with Pseudoexfoliation Syndrome

Xiaodong Zheng,<sup>1</sup> Atsushi Shiraishi,<sup>1</sup> Shinichi Okuma,<sup>1</sup> Shiro Mizoue,<sup>1</sup> Tomoko Goto,<sup>1,2</sup> Shiro Kawasaki,<sup>1</sup> Toshibiko Uno,<sup>1,3</sup> Tomoko Miyoshi,<sup>1,2</sup> Alfredo Ruggeri,<sup>4</sup> and Yuichi Ohashi<sup>1</sup>

**PURPOSE.** To measure the density of cells in different layers of the cornea and to determine whether morphologic changes of the subbasal corneal nerve plexus are present in eyes with the pseudoexfoliation (PEX) syndrome.

**METHODS.** Twenty-seven patients with unilateral PEX syndrome and 27 normal controls were investigated. All eyes underwent corneal sensitivity measurements with an esthesiometer and in vivo confocal microscopic study. Densities of the epithelial, stromal, and endothelial cells were measured. The density and tortuosity of the subbasal corneal nerve plexus were also evaluated.

**RESULTS.** Eyes with PEX syndrome had significantly lower cell densities in the basal epithelium ( $P = 0.003$ ), anterior stroma ( $P = 0.007$ ), intermediate stroma ( $P = 0.009$ ), posterior stroma ( $P = 0.012$ ), and endothelium ( $P < 0.0001$ ) than in the corresponding layers of normal eyes. PEX eyes also had lower subbasal nerve densities and greater tortuosity of the nerves than normal eyes. Fellow eyes of patients with PEX also had significantly lower densities of the basal epithelial and endothelial cells than the normal eyes. Corneal sensitivity was significantly decreased in PEX eyes, and this was significantly correlated with the decrease of basal epithelial cell and subbasal nerve densities.

**CONCLUSIONS.** These results have shed light on understanding of the pathogenesis of decreased corneal sensitivity in eyes with PEX syndrome. PEX syndrome is probably a binocular condition for which keratopathy of the fellow eye also requires observation. (*Invest Ophthalmol Vis Sci.* 2011;52:1755-1761) DOI:10.1167/iops.10-6098

The pseudoexfoliation (PEX) syndrome is a common age-related disorder of the extracellular matrix and is frequently associated with severe chronic secondary open angle glaucoma and cataract.<sup>1-3</sup> The prevalence of PEX syndrome varies widely in different racial and ethnic populations. In addition, the prevalence of PEX is dependent on the age and sex distribution of the population examined, the clinical criteria used to diagnose PEX, and the ability of the examiner to

detect early stages and more subtle signs of PEX. For example, the highest rates in studies of persons older than 60 years of age have been reported to be approximately 25% in Iceland and more than 20% in Finland.<sup>3,4</sup> The ocular manifestation of PEX syndrome is the production and progressive accumulation of abnormal extracellular fibrillar material in almost all the inner wall tissues of the anterior segment of the eye. This characteristic alteration predisposes the eye to a broad spectrum of intraocular complications including phacodonesis and lens subluxation, angle closure glaucoma, melanin dispersion, poor mydriasis, blood-aqueous barrier dysfunction, posterior synechiae, and other related complications.<sup>1-3</sup>

The PEX syndrome is associated with corneal endotheliopathy, and this has been suggested to be the cause of the so-called atypical non-guttata Fuchs endothelial dystrophy.<sup>5,6</sup> PEX endotheliopathy, a slowly progressing disease of the corneal endothelium, is usually bilateral but is often asymmetrical. It can lead to early corneal endothelial cell decompensation, which can then induce severe bullous keratopathy, a vision-threatening disorder.

Clinical signs of PEX syndrome include decreased corneal sensitivity, thinning of the central corneal thickness, and impaired tear film stability.<sup>7-9</sup> However, the underlying cause of these clinical findings has not been well investigated, possibly because objective and accurate in vivo examination techniques are not available.

Recent advances in imaging technology have improved the ability of these instruments to diagnose different ocular diseases. The Rostock Cornea Module (Heidelberg Engineering, Heidelberg, Germany), consisting of a contact lens system attached to the Heidelberg Retina Tomograph II (Heidelberg Engineering), is such an instrument. It uses laser scanning technology to investigate the cornea at a cellular level, and structures such as the subbasal nerve plexus, which cannot be seen by slit-lamp microscopy, can be clearly seen.<sup>10,11</sup>

In vivo confocal microscopy (IVCM) was used by Martone et al.<sup>12</sup> to examine one eye with PEX syndrome, and noncontact IVCM was used by Sbeity et al.<sup>13</sup> to study PEX, PEX-suspect, and normal eyes. However, there has not been a detailed and quantitative study of the morphologic changes in the corneas of eyes with PEX syndrome.

Thus, the purpose of this study was to examine the underlying pathogenesis of PEX keratopathy and to obtain evidence to explain clinical findings such as the decreased corneal sensitivities observed in patients with PEX syndrome. To accomplish this, we used IVCM to determine cell densities in different corneal layers of eyes with PEX syndrome and their clinically unaffected fellow eyes. These findings were compared with those in normal control eyes. The nerve densities in the subbasal layer were also analyzed, and their relationship with the alterations of clinical corneal sensitivity were analyzed.

From the <sup>1</sup>Department of Ophthalmology, Ehime University School of Medicine, Ehime, Japan; <sup>2</sup>Department of Ophthalmology, Takanoko Hospital, Ehime, Japan; <sup>3</sup>Department of Ophthalmology, Red Cross Hospital in Matsuyama, Ehime, Japan; and <sup>4</sup>Department of Information Engineering, University of Padua, Padua, Italy.

Submitted for publication June 22, 2010; revised October 8, 2010; accepted November 1, 2010.

Disclosure: X. Zheng, None; A. Shiraishi, None; S. Okuma, None; S. Mizoue, None; T. Goto, None; S. Kawasaki, None; T. Uno, None; T. Miyoshi, None; A. Ruggeri, None; Y. Ohashi, None

Corresponding author: Xiaodong Zheng, Department of Ophthalmology, Ehime University School of Medicine, Toon City, Ehime 791-0295, Japan; xzheng@m.ehime-u.ac.jp.

## SUBJECTS AND METHODS

### Subjects

We studied 27 patients (16 men, 11 women; mean age,  $74.4 \pm 6.3$  years; age range, 65–90 years) with diagnoses of unilateral PEX syndrome. In all eyes, exfoliation material (XFM) was seen by slit-lamp microscopy at the pupillary border or on the anterior lens capsule. Eyes with PEX syndrome were placed in the PEX group, and clinically normal fellow eyes were placed in the PEX fellow eye group. Age- and sex-matched normal subjects (16 men, 11 women; mean age,  $72.7 \pm 6.5$  years; age range, 61–92 years) were also studied. One eye from the normal control group was randomly selected and used in the statistical analyses. Exclusion criteria included Stevens-Johnson syndrome, lymphoma, sarcoidosis, corneal dystrophy, injury, inflammation, systemic therapy with drugs with known corneal toxicity; treatment with topical anti-glaucoma drugs, steroids, or NSAIDs; contact lens wear; previous ocular surgery; and other ophthalmic diseases.

The procedures used conformed to the tenets of the Declaration of Helsinki. Informed consent was obtained from all subjects after an explanation of the nature and possible consequences of the procedures. The protocol used was approved by the Ethics Committee of Ehime University School of Medicine.

### Corneal Sensitivity Measurements

Measurement of the corneal sensitivity was performed with a Cochet-Bonnet nylon thread esthesiometer, as described.<sup>14</sup> The examination was begun with a 60-mm length of nylon filament applied perpendicularly to the central cornea, and the tests were continued by shortening the filament by 5 mm each time until the subject felt the contact of the filament. Each subject was measured twice with a between-test interval of at least 5 minutes, and the average of two measurements was used for the statistical analyses.

### In Vivo Confocal Microscopy

IVCM was performed on all subjects with the Rostock Corneal Module of the Heidelberg Retina Tomograph II (HRTII-RCM; Heidelberg Engineering). After topical anesthesia with 0.4% oxybuprocaine (Santen Pharmaceuticals, Osaka, Japan), the subject was positioned in the chin and forehead holder and instructed to look straight ahead at a target to make sure that the central cornea was scanned. The objective of the microscope was an immersion lens (magnification  $\times 63$ ; Zeiss, Chester, VA) covered by a polymethylmethacrylate cap (TomoCap; Heidelberg Engineering). Comfort gel (Bausch & Lomb, Berlin, Germany) was used to couple the applanating lens cap to the cornea. The polymethylmethacrylate cap was applanated onto the center of the cornea by adjusting the controller, and in vivo digital images of the cornea were seen on the monitor screen. When the first layer of superficial epithelial cells was seen, the digital micrometer gauge was set to zero, and then a sequence of images was recorded as the focal plane was gradually moved toward the endothelium. Each subject underwent scanning three times at intervals of at least 15 minutes.

The laser source of the HRT-II RCM is a diode laser with a wavelength of 670 nm. Two-dimensional images consisting of  $384 \times 384$  pixels covering an area of  $400 \times 400 \mu\text{m}$  were recorded. The digital resolution was  $1.04 \mu\text{m}/\text{pixel}$  transversally and  $2 \mu\text{m}/\text{pixel}$  longitudinally, as stated by the manufacturer.

### Image Analyses

Central corneal images of all subjects were taken, and the three best-focused images from the superficial epithelium, basal epithelium, subbasal nerve plexus, anterior stroma, intermediate stroma, posterior stroma, and endothelium were selected for analyses. The selected images were randomly presented to two masked observers (XZ, SO) for evaluation. All data are presented as averages of three images.

### Cell Density Analyses

Morphologic characteristics and densities in the different layers of the cornea in the PEX and PEX fellow eyes were assessed and compared with those of normal controls. Superficial epithelial cells were identified as polygonal cells with clearly visible cell borders, bright cytoplasm, and dark nuclei. Basal epithelial cells were identified as the layer just above the amorphous-appearing Bowman membrane. Basal cells had bright borders, a uniform shape, and nonhomogeneous cytoplasm. The anterior stroma was identified as the first layer immediately beneath the Bowman membrane, and the posterior stroma was identified as the layer just anterior to the Descemet membrane and the endothelium. The intermediate stroma was defined as the layer halfway between the anterior and posterior stroma.<sup>15</sup> The corneal endothelium consisted of a monolayer of regularly arranged hexagonal cells with dark borders and bright reflecting cytoplasm.

After selecting a frame of the image and manually marking the cells inside the frame ( $>50$  cells), cell densities were calculated automatically by the software installed in the instrument. Cells partially contained in the area analyzed were counted only along the upper and right margins. The results are expressed in cells per square millimeter.

### Analyses of Subbasal Nerve Plexus

The subbasal nerve plexus layer is located between the Bowman membrane and the basal epithelial layer through which numerous nerve fibers pass. The density and tortuosity of the subbasal nerve plexus were analyzed as described.<sup>14,16</sup> Two parameters were analyzed: the long nerve fiber density (LNFD) was determined by dividing the number of long nerves by the image area ( $0.16 \text{ mm}^2$ ), and the nerve branch density (NBD) was determined by dividing the total number of long nerves and their branches by the image area. Nerve tortuosity was classified into 4 gradings: grade 1 = approximately straight nerves; grade 4 = very tortuous nerves with significant convolutions throughout their course.<sup>16</sup>

### Statistical Analyses

Data were analyzed with statistical software (JMP, version 8.0 for Windows; SAS Japan Inc., Tokyo, Japan). All data are expressed as the mean  $\pm$  SD. The differences of cell densities between PEX eyes and normal controls or between PEX fellow eyes and normal controls were evaluated with two-tailed Student's *t*-tests. The differences of cell densities between PEX eyes and their fellow eyes were evaluated by paired *t*-tests. The Wilcoxon rank sum test was used to compare the values of corneal sensitivity, LNFD, NBD, and the nerve tortuosity between PEX patients and normal controls. Spearman's correlation was used to determine the correlation among the parameters of basal epithelial cell density, subbasal nerve density, and corneal sensitivity.  $P < 0.05$  was considered statistically significant.

## RESULTS

The mean age was not significantly different between patients with PEX and normal controls (two-tailed Student's *t*-tests,  $P = 0.725$ ). Eyes with PEX showed typical whitish exfoliation material on the pupillary border or on the anterior lens capsule on slit-lamp examination. Pigmented keratoprecipitates and slight folding of Descemet membrane were also detected in some patients. Fellow eyes of PEX eyes and normal control eyes appeared normal by slit-lamp microscopy.

### Corneal Sensitivity

The mean corneal sensitivity was  $47.8 \pm 5.6$  mm for PEX eyes and  $53.7 \pm 4.9$  mm for PEX fellow eyes. This difference was significant ( $P = 0.005$ ; Wilcoxon rank sum test). Mean corneal

sensitivity was  $55.6 \pm 4.7$  mm for the normal control subjects, and the corneas of eyes with PEX were significantly less sensitive than those of normal control eyes ( $P < 0.0001$ ). The difference in corneal sensitivity between PEX fellow eyes and normal controls was not significant ( $P = 0.378$ ).

**Cell Densities**

The density of the corneal superficial epithelial cells was  $872.6 \pm 95.3$  cells/mm<sup>2</sup>, and that for the basal epithelial cells was  $4829.7 \pm 462.1$  cells/mm<sup>2</sup> in PEX eyes. Densities for the corresponding layers in PEX fellow eyes were  $910.4 \pm 80.8$  cells/mm<sup>2</sup> and  $4996.7 \pm 438.7$  cells/mm<sup>2</sup>, and densities for the normal control eyes were  $886.4 \pm 101.7$  cells/mm<sup>2</sup> and  $5446.4 \pm 639.9$  cells/mm<sup>2</sup>. The density of the basal epithelial cells was significantly lower for PEX eyes and PEX fellow eyes than for the control eyes ( $P = 0.003$  and  $P = 0.015$ , respectively; two-tailed Student's *t*-tests; Fig. 1). The difference in the density of the basal epithelial cells between PEX eyes and PEX fellow eyes was not significant ( $P = 0.589$ ; paired *t*-test). Differences in the densities of the superficial epithelial cells among the three experimental groups also were not significant (Fig. 1).

Densities of the cells in the three stromal layers of PEX eyes, PEX fellow eyes, and normal control eyes are shown in Figure 2. Compared with normal controls, the cell densities of PEX eyes were significantly lower in all three layers of the stroma (anterior stroma,  $P = 0.007$ ; intermediate stroma,  $P = 0.009$ ; posterior stroma,  $P = 0.012$ ; two-tailed Student's *t*-tests). The densities in these three stromal layers in PEX fellow eyes were also lower, but the decrease was not significant ( $P = 0.196$ ;  $P = 0.261$ ;  $P = 0.08$ ; respectively; Fig. 2).

Endothelial cell densities were  $2240.7 \pm 236.6$  cells/mm<sup>2</sup>,  $2386.6 \pm 200.8$  cells/mm<sup>2</sup>, and  $2738.7 \pm 233.2$  cells/mm<sup>2</sup> for PEX eyes, PEX fellow eyes, and normal eyes, respectively. Differences between PEX eyes and normal controls ( $P < 0.0001$ ; two-tailed Student's *t*-test; Fig. 1) and between PEX fellow eyes and normal controls were significant ( $P = 0.001$ ). The difference in endothelial cell density between PEX and PEX fellow eyes was not significant ( $P = 0.754$ ; paired *t*-test).

There was a higher degree of pleomorphism and polymegethism in PEX eyes than in control eyes. The coef-

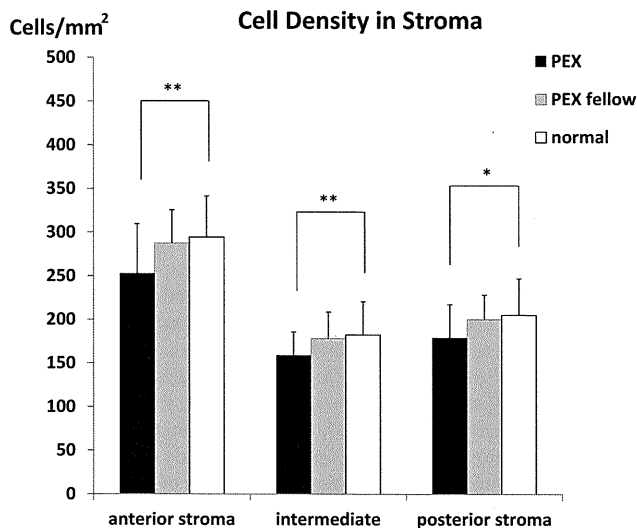


FIGURE 2. Cellular densities of anterior, intermediate and posterior stroma of eyes with PEX syndrome, their clinically unaffected fellow eyes, and eyes of normal control subjects. \*\* $P < 0.01$ ; \* $P < 0.05$ .

ficient of variation (CV) of the cell area was  $45.2\% \pm 8.7\%$ , and the percentage of hexagonal cells (HEX) in PEX eyes was  $30.5\% \pm 10.3\%$ . Both values are significantly different from those of normal control eyes (CV,  $30.6\% \pm 5.6\%$ ,  $P = 0.016$ ; HEX,  $50.3 \pm 6.8\%$ ,  $P = 0.008$ ; two-tailed Student's *t*-test). PEX fellow eyes also showed a similar tendency of increased pleomorphism and polymegethism, but the differences were not statistically significant.

**Subbasal Nerve Plexus**

The LNFD and NBD were significantly decreased in PEX eyes ( $17.4 \pm 6.3$  and  $32.2 \pm 8.3$  nerves/mm<sup>2</sup>, respectively) compared with those in normal controls ( $35.9 \pm 8.2$  and  $72.2 \pm 8.8$  nerves/mm<sup>2</sup>;  $P < 0.0001$  and  $P < 0.0001$ , respectively; Wilcoxon rank sum test; Fig. 3). PEX fellow eyes also had decreased LNFD and NBD, but these changes were not

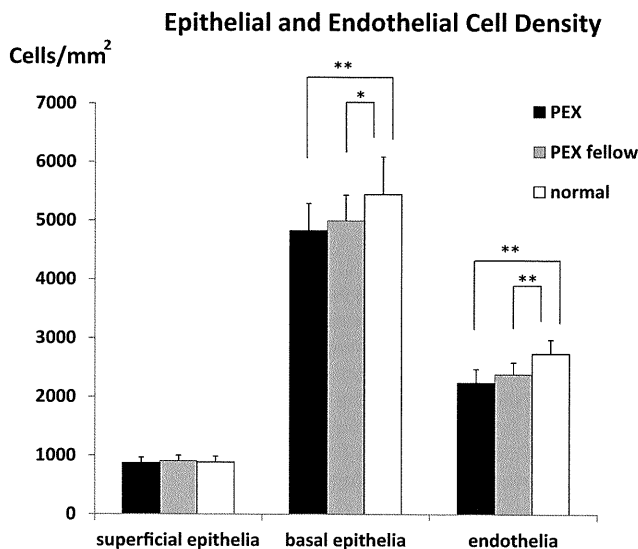


FIGURE 1. Corneal epithelial and endothelial cell densities of eyes with PEX syndrome, their clinically unaffected fellow eyes, and eyes of normal control subjects. \*\* $P < 0.01$ ; \* $P < 0.05$ .

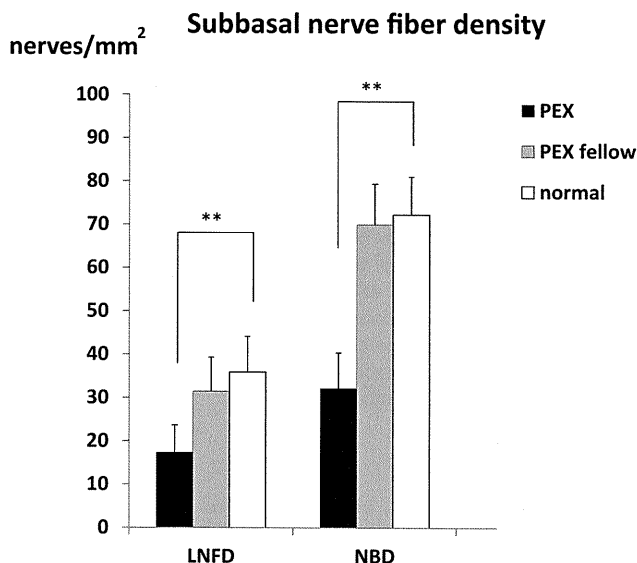
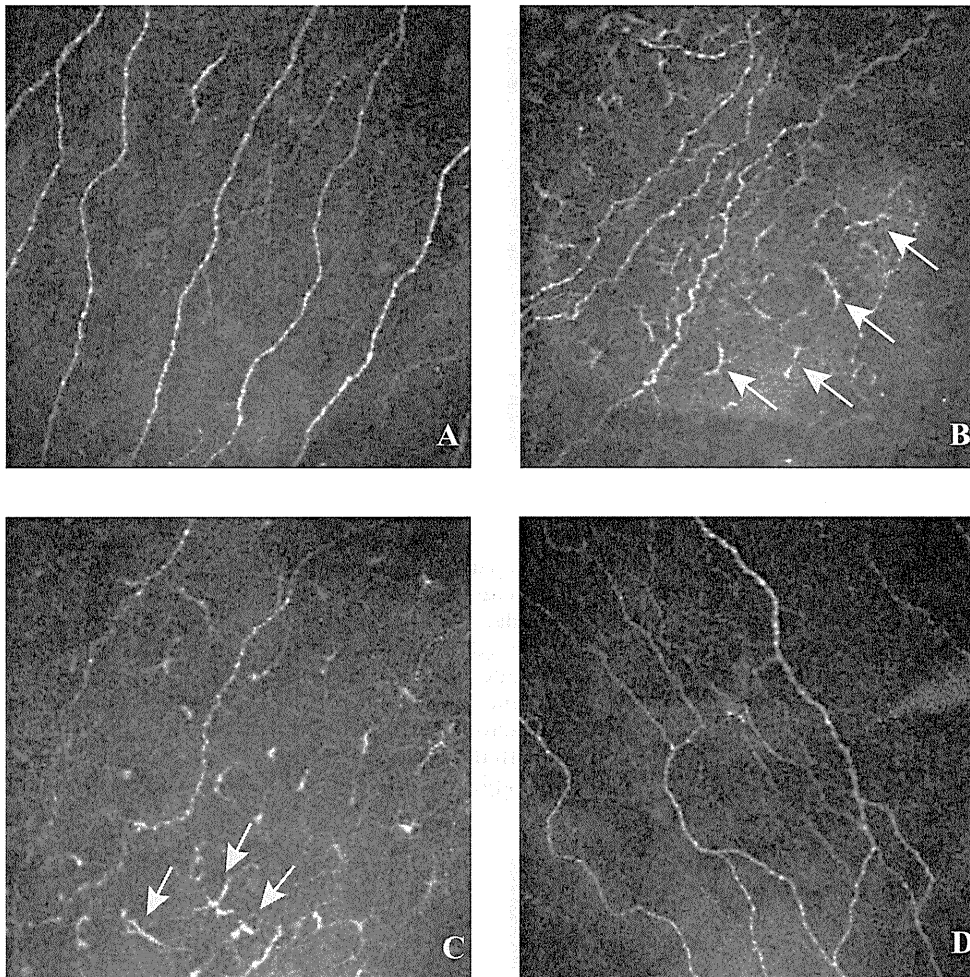


FIGURE 3. Subbasal LNFD and NBD in eyes with PEX syndrome, their clinically unaffected fellow eyes, and eyes of normal control subjects. \*\* $P < 0.01$ .



**FIGURE 4.** In vivo confocal microscopic images of the subbasal nerve plexus in patients with PEX syndrome and a normal control subject. (A) Representative image from a normal control subject showing subbasal nerve plexus with long nerve fibers running parallel to the Bowman layer. The nerve fibers appeared to be straight with minimal tortuosity. The subbasal LNFD was 31.3 nerves/mm<sup>2</sup>, and the nerve tortuosity was grade 1. (B) Representative image from a PEX syndrome eye showing very tortuous nerves with significant convolutions throughout their course. The tortuosity grade was 4. Note the intensive infiltration of dendritic cells (arrows) in close vicinity of the nerve fibers. (C) Confocal image of the subbasal nerve plexus of another PEX eye showing the thinning of the nerves, short nerve sprouts, fewer branches from the main nerve trunk, and significantly decreased nerve density. The LNFD was 6.3 nerves/mm<sup>2</sup>. Arrows: dendritic cell infiltration. (D) Confocal image of a PEX fellow eye showing moderately tortuous subbasal nerve plexus with a tortuosity grade of 3 and an LNFD of 18.8.

significantly different from those of the controls ( $31.5 \pm 7.8$  and  $69.9 \pm 9.4$  nerves/mm<sup>2</sup>;  $P = 0.093$  and  $P = 0.301$ ).

Confocal images of PEX eyes showed extremely tortuous nerve fibers, thinning of nerves, short nerve sprouts, fewer branches from the main nerve trunk, and highly reflective inflammatory infiltrates in close vicinity of the subbasal nerves. Representative confocal images of the three groups are shown in Figure 4. In PEX eyes, 85.2% (23 of 27 eyes) had grade  $\geq 3$  subbasal nerve tortuosity, and the degree of tortuosity in PEX eyes was significantly higher than that of the controls ( $3.2 \pm 0.7$  vs.  $1.6 \pm 0.6$ ;  $P < 0.0001$ ; Wilcoxon rank sum test). The degree of tortuosity in PEX fellow eyes was also greater than that of normal controls, although the difference was not significant ( $2.1 \pm 0.9$  vs.  $1.6 \pm 0.6$ ;  $P = 0.054$ ).

It was our impression that PEX eyes had more inflammatory cells, including dendritic cells, infiltrating the subbasal cell layer and anterior stroma, and these changes were more severe in eyes with decreased subbasal nerve densities and lower corneal sensitivities (Fig. 4).

#### Correlation between Corneal Sensitivity and Subbasal Nerve Density and Basal Epithelial Cell Density

Spearman's correlation analyses showed that there was a significant positive correlation between corneal sensitivity and the subbasal nerve densities (LNFD,  $r = 0.764$ ,  $P < 0.0001$ ; NBD,  $r = 0.634$ ,  $P < 0.0001$ ; Spearman correlation coefficient). Corneal sensitivity was also significantly and positively correlated with basal epithelial cell density and

significantly and negatively correlated with subbasal nerve tortuosity (Table 1).

#### Confocal Microscopic Detection of Hyperreflective Material

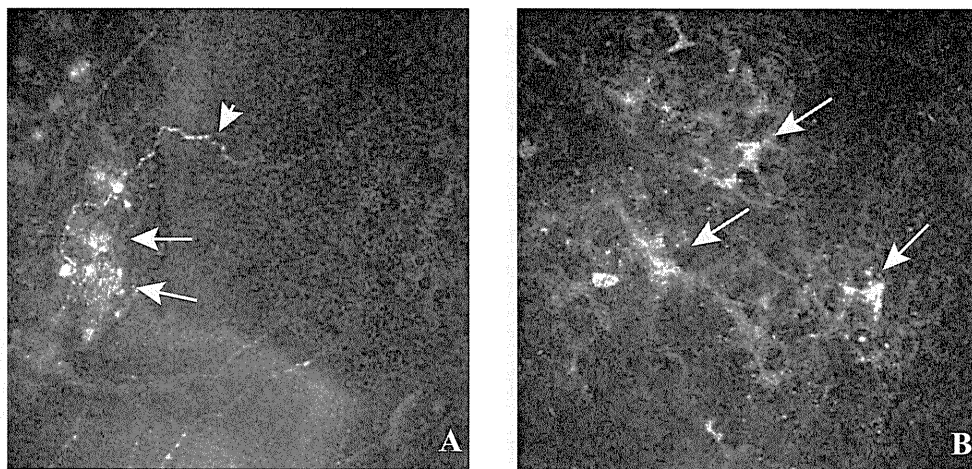
IVCM showed hyperreflective material, probably XFM, in the subbasal epithelial layer or the anterior stroma of 22 of the 27 PEX eyes (81.5%). The hyperreflective material was also observed abundantly in the endothelia of all PEX eyes. Five of 27 (18.5%) PEX fellow eyes showed hyperreflective deposits in the subbasal epithelial layer or anterior stroma, and 14 of 27 (51.9%) had endothelial surface deposits of hyperreflective material. In sharp contrast, none of the normal eyes showed hyperreflective material in the subbasal epithelial or anterior

**TABLE 1.** Correlation among Corneal Sensitivity, Subbasal Nerve Fiber Density, Tortuosity, and Basal Epithelial Cell Density

	Corneal Sensitivity	
	Spearman Correlation Coefficient	P
Long nerve fiber density	0.7640	<0.0001*
Nerve branch density	0.6341	<0.0001*
Subbasal nerve fiber tortuosity	-0.8250	<0.0001*
Basal epithelial cell density	0.6971	<0.0001*

\* Statistically significant.

**FIGURE 5.** Confocal microscopic images showing XFM in the subbasal nerve plexus layer of a patient with PEX syndrome. (A) Nerve fiber thinning with tortuous morphology can be seen (*arrowhead*), and XFM (*arrows*) is seen in close vicinity of the pathogenic nerve fibers. (B) Hyperreflective deposits (*arrows*) indicative of XFM can be seen in the subbasal amorphous layer of the cornea of another patient in the PEX eye group.



stromal layers, and only two (7.4%) had a small amount of hyperreflective material on the endothelial surface (Figs. 5, 6).

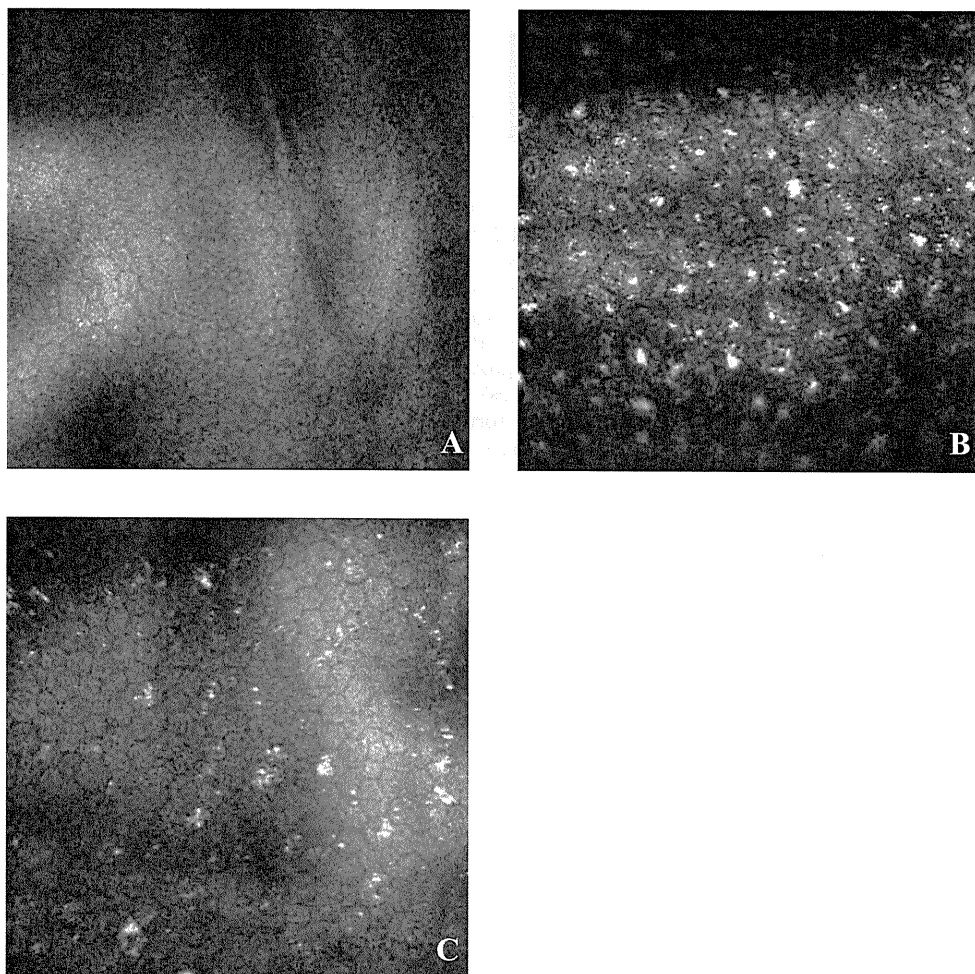
**DISCUSSION**

The manifestations of PEX syndrome in the anterior segment are widely known to affect intraocular surgery with poor mydriasis and intensive postoperative inflammation. The fact that aggregates of XFM can be identified in autopsy specimens of the heart, lung, liver, kidney, and other organs

in patients with ocular PEX suggests that the ocular PEX syndrome is part of a general systemic disorder.<sup>1-3,17</sup> In fact, PEX syndrome has been reported to be associated with cardiovascular diseases, chronic cerebral disorders, Alzheimer disease, and acute cerebrovascular events.<sup>1-3</sup> Two single nucleotide polymorphisms in the lysyl oxidase-like 1 (*LOXLI*) gene have been recently identified as strong genetic risk factors for PEX syndrome and PEX glaucoma.<sup>18</sup>

IVCM with the HRTII-RCM provides a new imaging method that allows rapid, noninvasive, high-resolution, and microstruc-

**FIGURE 6.** Representative confocal microscopic images of the endothelial layers of PEX syndrome eye, PEX fellow eye, and normal control eye group. (A) Normal subject with regularly arranged hexagonal endothelial cells. (B) PEX eye showing increases in pleomorphism and polymegethism and decrease in cell density. Intense hyperreflective materials indicative of XFM can be seen. (C) PEX fellow eye showing similar changes of endothelial cells and deposition of XFM.



tural examination of the cornea.<sup>10,11</sup> Only two studies have used IVCM to study the corneas of patients with PEX syndrome. Martone et al.<sup>12</sup> reported the findings in one case, and they reported that ICVM can detect hyperreflective deposits and dendritic cells infiltrating the basal epithelial cell layer. Fibrillar subepithelial structures were found, and the endothelial layer showed cellular anomalies. In a prospective observational case series, Sbeity et al.<sup>13</sup> used noncontact IVCM to detect XFM on the lens surfaces and corneal endothelia of PEX eyes and their fellow eyes.

Our study was the first to use IVCM to investigate cell densities in different layers of the cornea and to determine alterations of subbasal nerve density and tortuosity in PEX and PEX fellow eyes. Our results showed a significant decrease in the densities of the corneal endothelial cells in PEX eyes and their fellow eyes, which is in agreement with earlier observations by specular microscopy.<sup>8,19,20</sup> In addition, the clear confocal images allowed us to detect pleomorphisms and polymegathisms of the endothelial cells. All PEX eyes and 51.9% of PEX fellow eyes showed deposits of hyperreflective material in the endothelium, indicative of either pigment granules or XFM. In agreement with Sbeity et al.,<sup>13</sup> we believe that the pleomorphic and irregular deposits found on the corneal endothelium most likely represent XFM rather than pigment granules, which are round and uniform in size.<sup>13</sup> In addition, a number of patients who had no visible pigment keratoprecipitates on slit-lamp microscopy were found to have abundant large and irregular hyperreflective deposits on the endothelium in the confocal images.

PEX syndrome-associated corneal endotheliopathy has been suggested to be caused by one or a combination of the following alterations: hypoxic changes in the anterior chamber, accumulation of extracellular matrix, fibroblastic changes of the endothelium, and increased concentration of TGF- $\beta$ .<sup>1-3</sup> Our confocal microscopic findings suggest that the XFM, possibly at different stages of the normal course of PEX, may be deposited on the endothelium or may migrate from the endothelial cells that undergo fibroblastic changes. Our findings also showed that hyperreflective materials are found not only on the endothelium of PEX eyes but also in their fellow eyes, indicating that the fellow eyes might be at a preclinical stage of PEX syndrome. A bilateral decrease in the endothelial cell counts and morphologic alterations of endothelium support the idea that PEX is a binocular and systemic abnormality. Patients with unilateral PEX syndrome may have asymmetric manifestation of this slowly progressing disease.

Of clinical significance was our finding that the decreased stromal cell densities observed by IVCM could possibly explain the report that the central corneas of PEX eyes were thinner than those of normal subjects.<sup>8</sup> The pathogenesis of the decrease of stromal cell density in PEX eyes warrants future study. Because XFM deposits were simultaneously observed in the anterior stroma of PEX eyes, we suggest that the XFM may be somehow causative for this alteration, perhaps by inducing apoptosis of the keratocytes. Other pathogenic factors, such as altered levels of cytokines or chemokines in the cornea, could also be responsible, and this definitely warrants future investigation. In addition, PEX fellow eyes also had lower cell counts in the stroma, although the difference was not statistically significant. We suggest that the cause of the binocular differences in our study might have been because the two eyes were at different stages of the PEX process, and PEX fellow eyes may still be at a preclinical stage of PEX syndrome.

Other important findings were found in the subbasal nerve plexus. Our results showed that the subbasal nerve density was significantly lower and the nerves were mostly tortuous, with beading and thinning in PEX eyes. Interestingly, PEX fellow eyes also had similar alterations, though the changes were not

significant. These findings support the idea that PEX syndrome is a binocular abnormality that is expressed in both eyes but to different degrees. The important clinical significance of our study is that our correlation analyses showed that the decreased subbasal nerve density and increased tortuosity were significantly correlated with decreased corneal sensitivity. These results provide evidence, for the first time, that the cause of the decreased corneal sensitivity in eyes with PEX syndrome is the decreased subbasal nerve density. For patients with PEX syndrome, it would be practical and feasible to examine corneal sensitivity to assess the severity of PEX keratopathy and perhaps to predict the progression of PEX syndrome. In addition, detection of the morphologic changes in cell densities and subbasal nerve abnormalities by IVCM in the fellow eyes indicates that it is a sensitive tool for the diagnosis of preclinical stage of PEX syndrome. Our findings showed that PEX keratopathy may develop before any clinically visible XFM deposits are detected on the lens capsule or iris. If these findings are confirmed, then keratopathy may be the first event of the ocular complications of PEX syndrome. These findings also indicate that clinically unaffected fellow eyes of patients with PEX syndrome are probably at risk for PEX syndrome, and more frequent ophthalmologic examinations are necessary.

This study has increased our understanding of the keratopathy of this most likely systemic abnormality. Whether the alternations of the subbasal corneal nerves are primary or secondary changes of the disease must be determined. Because of the increase in the elastic microfibril components and imbalances in the matrix metalloproteinases (MMPs) and tissue inhibitors of MMP in eyes with PEX syndrome, PEX fibrils accumulate in the tissues.<sup>1-3</sup> Our findings that XFM deposits were frequently observed close to the subbasal epithelial layer or anterior stroma support the idea that besides an abnormal aggregation of elastic microfibrils into exfoliation fibers (the elastic microfibril hypothesis),<sup>1-3,21</sup> other extracellular matrix components, such as basement membrane components, may possibly interact and become incorporated into the composite XFM (the basement membrane hypothesis).<sup>2,3</sup> In addition, our observation of an infiltration of dendritic cells in close vicinity of the subbasal nerve plexus layer indicates the possibility that accumulation of extracellular XFM may induce inflammatory responses, which then recruit antigen-presenting cells such as immunocompetent dendritic cells. This excessive deposition of XFM and infiltration of dendritic cells may play a role in the neuropathy of the subbasal nerve plexus, resulting in decreased corneal sensitivity in patients with PEX syndrome.

Some limitations were present in this study. First, the IVCM scans a very small area of the cornea, which may generate biases among different portions of scanning of different groups. As mentioned, efforts were taken to scan the center of the cornea of each subject. In addition, we also confirmed our findings by scanning the midperipheral and peripheral portions of the cornea (data not shown).

Second, IVCM images may not represent the true histologic changes of the cornea. By applying the same criteria for image evaluation, we can conclude that the differences between the studied groups were still detected. Furthermore, it was our impression that fewer keratocytes were seen in the stromas of corneal specimens obtained from PEX syndrome patients with penetrating keratoplasty.

Future investigations, including a thorough and quantitative analysis of the exfoliation material by confocal imaging, are needed. In addition, the correlations between IVCM findings with endothelial barrier function should be determined. If the confocal findings can provide clues for preclinical stages of endothelial barrier dysfunction of the cornea in PEX syndrome, their clinical significance can be used in designing an early treatment protocol.

In summary, our study demonstrated that eyes with PEX syndrome have decreased cell densities in the cornea. The subbasal nerve density was also significantly decreased, and this was significantly correlated with clinically decreased corneal sensitivity. Our study sheds light on understanding the cause of impaired corneal sensitivity in patients with PEX syndrome. The PEX syndrome is probably a bilateral event in which the keratopathy of the fellow eye also must be observed.

## References

1. Naumann GOH, Schlötzer-Schrehardt U, Kuchle M. Pseudoexfoliation syndrome for the comprehensive ophthalmologist: intraocular and systemic manifestations. *Ophthalmology*. 1998;105:951-968.
2. Schlötzer-Schrehardt U, Naumann GOH. Ocular and systemic pseudoexfoliation syndrome. *Am J Ophthalmol*. 2006;141:921-937.
3. Ritch R, Schlötzer-Schrehardt U. Exfoliation syndrome. *Surv Ophthalmol*. 2001;45:265-315.
4. Forsius H. Prevalence of pseudoexfoliation of the lens in Finns, Lapps, Icelanders, Eskimos, and Russian. *Trans Ophthalmol Soc UK*. 1979;99:296-298.
5. Naumann GOH, Schlötzer-Schrehardt U. Keratopathy in pseudoexfoliation syndrome as a cause of corneal endothelial decompensation—a clinicopathologic study. *Ophthalmology*. 2000;107:1111-1124.
6. Abbott RL, Fine BS, Webster RB Jr, et al. Specular microscopic and histologic observations in nonguttata corneal endothelial degeneration. *Ophthalmology*. 1981;88:788-800.
7. Detorakis ET, Koukoulas S, Chrisochou F, Konstas AG, Kozobolis VP. Central corneal mechanical sensitivity in pseudoexfoliation syndrome. *Cornea*. 2005;24:688-691.
8. Inoue K, Okugawa K, Oshika T, Amano S. Morphological study of corneal endothelium and corneal thickness in pseudoexfoliation syndrome. *Jpn J Ophthalmol*. 2003;47:235-239.
9. Kozobolis VP, Christodoulakis EV, Naoumidi II, Siganos CS, Detorakis ET, Pallikaris LG. Study of conjunctival goblet cell morphology and tear film stability in pseudoexfoliation syndrome. *Graefes Arch Clin Exp Ophthalmol*. 2004;42:478-483.
10. Patel DV, McGhee CNJ. In vivo confocal microscopy of human corneal nerves in health, in ocular and systemic disease, and following corneal surgery: a review. *Br J Ophthalmol*. 2009;93:853-860.
11. Guthoff RF, Zhivov A, Stachs O. In vivo confocal microscopy, an inner vision of the cornea—a major review. *Clin Exp Ophthalmol*. 2009;37:100-117.
12. Martone G, Casprini F, Traaversi C, Lepri F, Picherri P, Caporossi A. Pseudoexfoliation syndrome: in vivo confocal microscopy analysis. *Clin Exp Ophthalmol*. 2007;35:582-585.
13. Sbeity Z, Palmiero PM, Tello C, Liebmann JM, Ritch R. Non-contact in vivo confocal scanning laser microscopy in exfoliation syndrome, exfoliation syndrome suspect and normal eyes. *Acta Ophthalmol*. 2009 Oct 23 [Epub ahead of print].
14. Hu Y, Matsumoto Y, Adan ES, et al. Corneal in vivo confocal scanning laser microscopy in patients with atopic keratoconjunctivitis. *Ophthalmology*. 2008;115:2004-2012.
15. Quadrado MJ, Popper M, Morgado AM, Murta JN, Best JAV. Diabetes and corneal cell densities in humans by in vivo confocal microscopy. *Cornea*. 2006;25:761-768.
16. Mocan MC, Durukan I, Irkec M, Orhan M. Morphologic alterations of both the stromal and subbasal nerves in the corneas of patients with diabetes. *Cornea*. 2006;25:769-773.
17. Schlötzer-Schrehardt U, Koca M, Naumann GOH, Volkholz H. Pseudoexfoliation syndrome: ocular manifestation of a systemic disorder? *Arch Ophthalmol*. 1992;110:1752-1756.
18. Thorleifsson G, Magnusson KP, Sulem P, et al. Common sequence variants in the LOXL1 gene confer susceptibility to exfoliation glaucoma. *Science*. 2007;317:1397-1400.
19. Wang L, Yamasita R, Hommura S. Corneal endothelial changes and aqueous flare intensity in pseudoexfoliation syndrome. *Ophthalmologica*. 1999;213:318-391.
20. Miyake K, Matsuda M, Inaba M. Corneal endothelial changes in pseudoexfoliation syndrome. *Am J Ophthalmol*. 1989;108:49-52.
21. Streeten BW, Gibson SA, Dark AJ. Pseudoexfoliative material contains an elastic microfibrillar-associated glycoprotein. *Trans Am Ophthalmol Soc*. 1986;84:304-320.

# Anterior Segment Optical Coherence Tomography Analysis of Clinically Unilateral Pseudoexfoliation Syndrome: Evidence of Bilateral Involvement and Morphologic Factors Related to Asymmetry

Xiaodong Zheng,<sup>1</sup> Hiroshi Sakai,<sup>2</sup> Tomoko Goto,<sup>1,3</sup> Koji Namiguchi,<sup>1</sup> Shiro Mizoue,<sup>1</sup> Atsushi Shiraiishi,<sup>1</sup> Shoichi Sawaguchi,<sup>2</sup> and Yuichi Ohashi<sup>1</sup>

**PURPOSE.** To compare the morphology of the anterior chamber angle (ACA) and iris in eyes with pseudoexfoliation (PEX) syndrome to that of their clinically unaffected fellow eyes and normal control eyes.

**METHODS.** Forty-two patients with unilateral PEX syndrome and 42 normal subjects were studied. Eyes were separated into those with PEX, their clinically unaffected fellow eyes, and normal eyes. The dark-light changes of the ACA and iris were documented by anterior segment optical coherence tomography (AS-OCT) video recordings. The nasal ACA parameters including the angle opening distance at 500  $\mu\text{m}$  (AOD500), the trabecular-iris space at 500  $\mu\text{m}$  (TISA500), and the trabecular-iris angle at 500  $\mu\text{m}$  (TIA500); anterior chamber depth (ACD); iris-lens contact distance (ILCD), and iris configuration were analyzed with the built-in software and a customized program.

**RESULTS.** The ACA parameters were not significantly different among all three groups in the dark. The PEX eyes had significantly smaller ACA parameters than their fellow eyes and normal control eyes in the light. PEX eyes also had significantly shallower ACD, longer ILCD, and greater iris convexity (both in dark and light), and thinner iris (in dark) than their fellow eyes. The fellow eyes had significantly lower ACD both in the dark and light, and smaller angle opening distance at 500  $\mu\text{m}$  and ILCD in the light than normal controls. There were no significant differences in the iris area among the three groups.

**CONCLUSIONS.** Differences in the anterior segmental morphology are present between PEX and fellow eyes. These disparities may be related to the asymmetry in patients with the unilateral PEX syndrome. (*Invest Ophthalmol Vis Sci.* 2011;52:5679-5684) DOI:10.1167/iovs.11-7274

The pseudoexfoliation (PEX) syndrome is a common age-related disorder of the extracellular matrix that can affect 10%–20% of people older than 60 years worldwide.<sup>1,2</sup> The main ocular manifestation of PEX is the production and pro-

gressive accumulation of abnormal extracellular fibrillar and pseudoexfoliation material in almost all of the inner walls of the anterior segment of the eye. There has been a renewed interest in this disease because of the better awareness of the complications accompanying PEX including phacodonesis and lens subluxation, intractable glaucoma, melanin dispersions, poor mydriasis, blood-aqueous barrier dysfunction, and posterior synechiae.<sup>1,2</sup>

Up to 76% of patients with PEX are initially diagnosed as having unilateral PEX.<sup>3</sup> However in an electron microscopic study, Parekh et al. reported that 26 of 32 patients (81%) with clinically unilateral PEX had pseudoexfoliation material on either the lens capsule or conjunctival samples of the clinically unaffected eyes.<sup>4</sup> Furthermore, several reports on the follow-up of patients with unilateral PEX documented that 74% to 81.6% of the unilateral cases became bilateral.<sup>5-7</sup> This suggested that unilateral PEX is in fact a bilateral but asymmetric condition, and the percentage of unilateral disease decreases with a corresponding increase in bilateral disease with increasing age. The factors affecting the conversion from unilateral to bilateral disease are not known, and the pathogenic mechanism underlying the asymmetric condition has not been determined. Subtle differences in ocular blood flow,<sup>8</sup> aqueous humor dynamics, blood-aqueous barrier function, or anterior segmental morphology might be responsible for the asymmetry.<sup>1,2</sup>

Ultrasound biomicroscopic (UBM) studies on the morphologic alterations of the anterior segment of PEX eyes have shown abnormalities of the zonules, lens thickening, shallow central anterior chamber depth (ACD), and occludable angles.<sup>9-14</sup> In unilateral PEX patients, the PEX eyes and fellow eyes have been reported to share some similar morphologic changes.<sup>14</sup>

With the advancement of ophthalmic imaging instruments, more information has been obtained on the morphology of the structures in different ocular disorders. Fourier domain anterior segment optical coherence tomography (AS-OCT) is a representative imaging technique that provides cross-sectional views of the anterior segment with a resolution better than that of UBM.<sup>15</sup> Images and measurements of very fine structures can be achieved rapidly and noninvasively. In addition, using the AS-OCT video mode has allowed investigators to document dynamic morphologic alterations of the anterior chamber angle (ACA) and iris during pupillary movements without being influenced by accommodation.<sup>16-18</sup>

The purpose of this study was to compare the morphology of the anterior segment of affected eyes and their fellow eyes in cases of unilateral PEX. To accomplish this, we recorded images of the anterior segment by AS-OCT during pupillary dilation and constriction. Comparisons were made of the ACA

From the <sup>1</sup>Department of Ophthalmology, Ehime University School of Medicine, Toon City, Ehime, Japan; <sup>2</sup>Department of Ophthalmology, University of the Ryukyus Hospital, Okinawa, Japan; and <sup>3</sup>Department of Ophthalmology, Takanoko Hospital, Matsuyama, Ehime, Japan.

Submitted for publication January 25, 2011; revised March 16, 2011; accepted April 19, 2011.

Disclosure: X. Zheng, None; H. Sakai, None; T. Goto, None; K. Namiguchi, None; S. Mizoue, None; A. Shiraiishi, None; S. Sawaguchi, None; Y. Ohashi, None

Corresponding author: Xiaodong Zheng, Department of Ophthalmology, Ehime University School of Medicine, Ehime 791-0295, Japan; xzheng@m.ehime-u.ac.jp.

and the iris parameters in the PEX eyes, their fellow eyes, and normal control eyes.

## SUBJECTS AND METHODS

### Patients and Control Subjects

We studied 45 consecutive patients with unilateral PEX syndrome who visited the Department of Ophthalmology, Ehime University from January 2009 to November 2010. All eyes were examined by slit-lamp biomicroscopy after pupillary dilation. PEX eyes had clinically evident PEX material at the pupillary border or on the anterior lens capsule in one eye. These eyes were placed in the PEX eye group. Their clinically unaffected fellow eyes were placed in the fellow eye group. Forty-five age- and sex-matched normal subjects were also studied and one eye was randomly selected as the normal control.

The exclusion criteria included: prior intraocular surgery, e.g., laser trabeculoplasty, laser iridotomy, laser iridoplasty, or ocular trauma; evidence of peripheral anterior synechiae on indentation; iris dystrophy or dyscoria; lymphoma, sarcoidosis, diabetic mellitus, inflammation; eyes using anti-glaucoma medications or having abnormal intraocular pressure; or use of systemic medications that could affect the ACA or pupillary reflex.

All participants underwent a complete ophthalmic examination, including best-corrected visual acuity, autorefraction, slit-lamp microscopy, and intraocular pressure measurements by applanation tonometry (Goldmann; Haag-Streit, K oniz, Switzerland). The ocular axial length was measured (IOL Master; Carl Zeiss, Jena, Germany). Gonioscopy was performed with a 4-mirror lens at high magnification ( $\times 16$ ) with the eye in the primary position of gaze. All investigated eyes had open-angles and all structures anterior to the scleral spur were identified by gonioscopy (Shaffer grade  $\geq 2$ ).

The procedures used conformed to the tenets of the Declaration of Helsinki. An informed consent was obtained from all subjects after an explanation of the nature and possible consequences of the procedures. The protocol used was approved by the Ethics Committee of Ehime University School of Medicine.

### Anterior Segment Optical Coherence Tomography

An experienced operator who was masked to the results of the ophthalmic examinations performed the AS-OCT (Swept-source 1000

CASIA AS-OCT, Tomey, Nagoya, Japan). This AS-OCT system had a 30 kHz axial scan rate with an axial resolution of 10  $\mu\text{m}$ . The use of 1310 nm wavelength coupled with high resolution Fourier domain-OCT improved the resolution and penetration of the measuring beam into turbid tissues with a scan depth of 6 mm. This was sufficient to image the entire anterior segment in one frame.<sup>15</sup> The scan of the anterior chamber was a noncontact procedure during which the subject fixated on an internal target.

The AS-OCT real-time video recording mode (4 frames per second) was used to study the changes of the ACA and the iris during pupillary dilation and light-induced constriction. The scan was centered on the pupil, and the scan passed along the nasal-temporal axis, i.e.,  $0^\circ$  to  $180^\circ$ . After one minute at 50 lux of dark-adaptation, a LED pen light (Gentos, Tokyo, Japan), fixed at a distance of 20 cm,  $45^\circ$  from the optic axis of the examined eye, was turned on. The illuminance of the light was standardized at 2000 lux, and it was kept on for 4 seconds to induce pupillary constriction. AS-OCT scans were recorded for 10 seconds and the operator chose the best video frame with good centering to analyze. Data were excluded if the scleral spur could not be identified or the frame was of suboptimal quality because of blinks and eye movements. Each eye was examined three times with an intertest interval of at least 10 minutes.

### Image Processing

All images were processed separately and analyzed by two observers (XZ and KN) who were masked to the clinical findings of the eye. The video file was reviewed and one frame of the images in the dark (most dilated pupil) and the light (most constricted pupil) were selected for each subject. The morphology of structures on the nasal side of the eye was analyzed. Images were first analyzed with the built-in software for the ACA parameters: angle opening distance at 500  $\mu\text{m}$  (AOD500), trabecular-iris space at 500  $\mu\text{m}$  (TISA500), and trabecular-iris angle at 500  $\mu\text{m}$  (TIA500). The central anterior chamber depth (ACD) and the pupillary diameter were also measured (Fig. 1A).

All images were then exported and analyzed with a customized software program written for the following iris parameters (Fig. 1B): the iris thickness in the dilator muscle region (DMR) which was set at one-half of the distance between the scleral spur and the pupillary margin was measured as described<sup>19</sup>; and the iris thickness in the sphincter muscle region (SMR) which was set at 0.75 mm from the pupillary margin was also measured. The ratio of the thickness at

### AS-OCT Analyses of Anterior chamber Angle and Iris Configuration

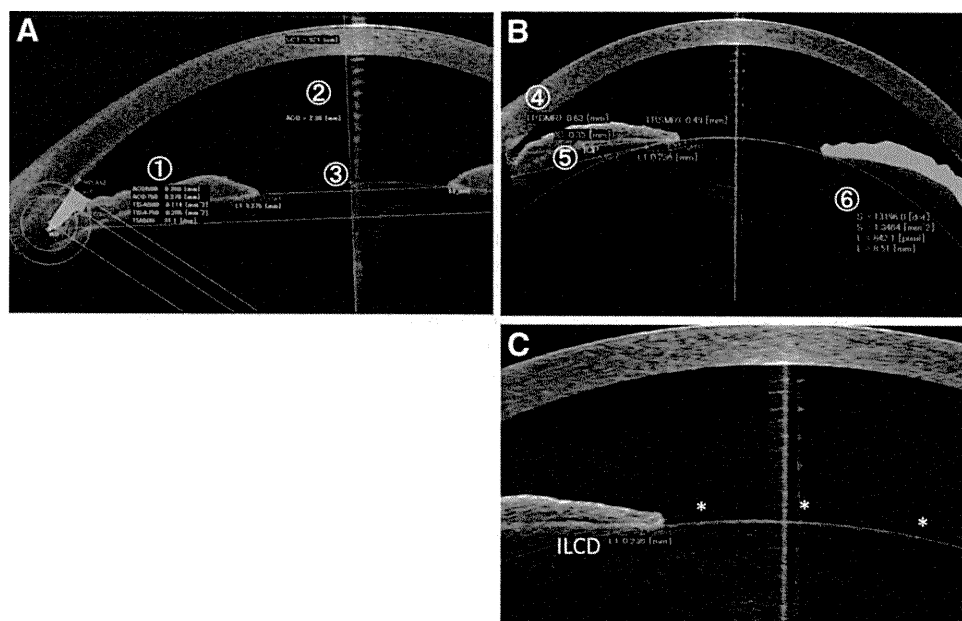


FIGURE 1. Anterior segment optical coherence tomographic (AS-OCT) images from which the morphologic parameters of the structures in the anterior chamber and the iris were measured. (A) Anterior chamber parameters of (1) angle opening distance at 500  $\mu\text{m}$  (AOD500), (2) central anterior chamber depth (ACD), and (3) pupillary diameter. (B) Iris configurations of (4) iris thickness (IT) at the dilator muscle region (DMR) measured at one-half of the distance between the scleral spur (SS) and the pupillary margin; iris thickness at the sphincter muscle region (SMR) measured at 0.75 mm from the pupillary margin, (5) iris convexity (IC), and (6) iris area (indicated by green shading over the right half of the iris). (C) Iris-lens contact distance (ILCD) measurement. Asterisks represent three points selected on the lens surface for generating estimated curved line of the anterior lens capsule. The ILCD was measured along the iris pigment epithelium from the papillary border to the point at which the iris was seen to separate from the anterior lens capsule.

the DMR and SMR (DMR/SMR) was used for the statistical analyses to reduce the intersubject variability.

In addition, the iris convexity was defined as the distance between the posterior point of greatest iris curvature to a line drawn from the most peripheral to the most central points of the iris pigment epithelium. The area of the iris was determined by the cumulative cross-sectional area of the iris from the scleral spur to the edge of the pupil.<sup>20</sup> A program was also written for the calculation of iris-lens contact distance (ILCD). To measure this, 3 points were manually designated on the lens surface and a curved line of the anterior lens capsule was automatically generated by the software. The ILCD was measured along the iris pigment epithelium from the pupillary border to the point at which the iris was seen to separate from the anterior lens capsule (Fig. 1C). These measurements had good reliability with the intraobserver and interobserver intraclass correlation coefficients ranging between 0.96 to 0.98 and 0.97 to 0.99, respectively.

**Statistical Analyses**

All data are expressed as the means ± standard deviations (SDs). Gender differences between PEX patients and normal subjects were evaluated by the  $\chi^2$  test. Comparisons of other demographic data, biometric characteristics, and AS-OCT parameters were evaluated by paired *t*-tests (PEX eye versus fellow eye) or two-tailed Student's *t*-tests (PEX eye versus normal control eye or fellow eye versus normal control eye). The ACA and iris parameters were compared with adjustment for pupil size. The significance of the differences in the DMR/SMR ratio among the three groups was determined by the Tukey-Kramer test. A probability level of *P* < 0.05 was considered statistically significant. Data were analyzed with statistical software (JMP version 9.0 for Windows; SAS Japan Inc., Tokyo, Japan).

**RESULTS**

Three patients with unilateral PEX and three normal subjects were excluded due to a poor imaging of the scleral spur. Forty-two patients (17 men and 25 women with a mean age of 72.7 ± 7.4 years and a range of 61 to 92 years) and 42 normal subjects (16 men and 26 women with a mean age of 73.6 ± 8.9 years and a range of 64 to 90 years) were analyzed. The mean age of the PEX patients was not significantly different from that of the normal controls (*P* = 0.886, two-tailed Student's *t*-test). Slit-lamp biomicroscopy showed that all eyes with PEX had typical whitish exfoliation material at the pupillary edge and on the anterior lens capsule. The fellow eyes and normal control eyes did not have these deposits. The differences in the visual acuity, gender distribution, refractive error (spherical equivalent), axial length, intraocular pressure, and gonioscopic grading (Shaffer) of the ACA among the three groups were not significant. The data are summarized in Table 1.

**Comparisons of AOD 500 for PEX, Fellow and Normal Control Eyes**

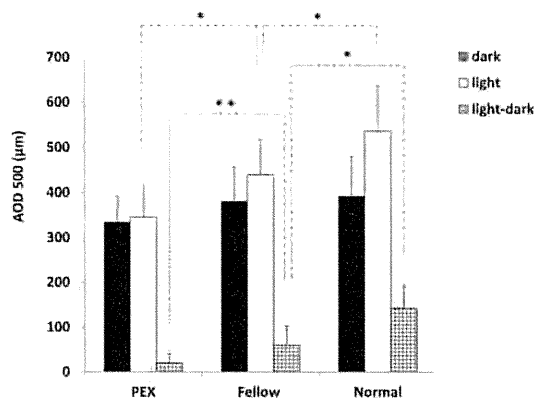


FIGURE 2. Comparisons of AOD500 for eyes with the PEX syndrome, their unaffected fellow eyes, and normal control eyes. Dark, values measured in the dark when pupils were mostly dilated; Light, values measured in the light when pupils were mostly constricted; Light-dark, AOD500<sub>(light)</sub> - AOD500<sub>(dark)</sub>. Statistical significance is denoted by \*\**P* < 0.01, and \**P* < 0.05.

**Anterior Chamber Angle (ACA) Morphology**

In the dark when pupils were dilated, the mean AOD500 was 333.6 ± 56.5 µm in the PEX eyes, 380.1 ± 76.4 µm in the fellow eyes, and 392.6 ± 87.2 µm in the normal control eyes (Fig. 2). The differences between the three groups were not significant (PEX versus fellow, *P* = 0.225, paired *t*-tests; PEX versus normal, *P* = 0.133; and fellow versus normal, *P* = 0.416, both two-tailed Student's *t*-test). When the pupils were constricted by light, the AOD500 in the PEX eyes was significantly smaller than that of the fellow eyes (*P* = 0.021) and the normal eyes (*P* = 0.008). The AOD500 in the fellow eyes was also significantly smaller than that of the normal eyes (*P* = 0.037). In addition, the mean dark-to-light change of the AOD500 for the PEX eyes was also significantly less than that of the fellow eyes (20.5 ± 16.6 µm vs. 60.8 ± 42.2 µm; *P* = 0.007) and of the normal control eyes (*P* = 0.004). The difference in the changes of the AOD500 between the fellow and normal control eyes was also significant (*P* = 0.033).

In the dark, the TISA500 was not significantly different among the three groups. However in light, the TISA500 of the PEX eyes was significantly smaller than that of the fellow eyes and normal control eyes (Fig. 3). In the light, the PEX eyes also had significantly narrower TIA500 than that of the fellow and normal control eyes. Similarly, the dark-to-light change of the TIA500 of the PEX eyes was significantly less than that of the

TABLE 1. Demographic and Biometric Characteristics of PEX Eye, Fellow Eye, and Normal Control Eye Groups

	PEX	Fellow	Normal	<i>P</i>
Age, y	72.7 ± 7.4	—	73.6 ± 8.9	0.886*
Sex, male/female	17/25	—	16/26	0.763†
Spherical equivalent, D	-0.34 ± 2.8	-0.22 ± 1.76	-0.28 ± 1.52	0.521‡
BCVA, LogMAR	0.04 ± 0.05	0.03 ± 0.04	0.00 ± 0.03	0.554‡
Axial length, mm	23.71 ± 0.94	24.06 ± 0.81	24.5 ± 1.01	0.669‡
Intraocular pressure, mm Hg	14.8 ± 3.1	13.6 ± 3.8	13.1 ± 4.8	0.375‡
Gonioscopy grading (Shaffer)	2.9 ± 0.68	3.1 ± 0.77	3.1 ± 0.82	0.428‡

Data are given as mean ± SD. All groups, *n* = 42. BCVA, best-corrected visual acuity; D, Diopter; LogMAR, logarithm of the minimum angle of resolution.

\* PEX patients versus normal control subjects (two-tailed Student's *t*-test).

† PEX patients versus normal control subjects ( $\chi^2$ ).

‡ PEX eye versus fellow eye (paired *t*-test).

## Comparisons of TISA 500 for PEX, Fellow and Normal Control Eyes

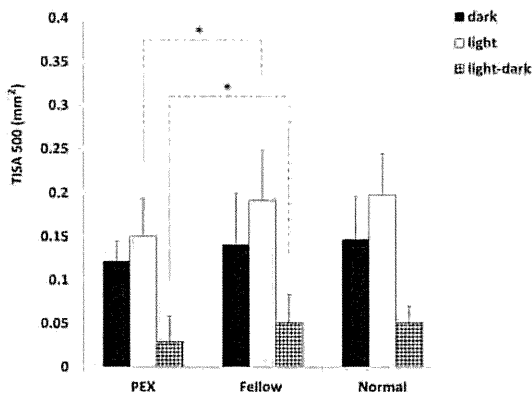


FIGURE 3. Comparisons of TISA500 for eyes with the PEX syndrome, their unaffected fellow eyes, and normal control eyes. Dark, values measured in the dark when pupils were mostly dilated; Light, values measured in the light when pupils were mostly constricted; Light-dark,  $TISA500_{(light)} - TISA500_{(dark)}$ . Statistical significance is denoted by  $*P < 0.05$ .

fellow eyes (Fig. 4). The PEX eyes had significantly smaller ACD than that of the fellow eyes both in dark and light ( $P = 0.021$  and  $P = 0.018$ , respectively; paired  $t$ -tests; Table 2). The ACD of the fellow eyes was also significantly smaller than that of normal control eyes ( $P = 0.038$  and  $P = 0.032$  for dark and light respectively; two-tailed Student's  $t$ -test).

The pupillary diameter in dark for the PEX eyes was significantly smaller than that of fellow eyes ( $P = 0.011$ ). When the dark-to-light change was analyzed, the PEX eyes had significantly less pupillary change than that of the fellow eyes ( $P = 0.025$ ) and the normal control eyes ( $P = 0.008$ ).

## Iris Configuration

The difference in the area of the iris was not significant among the three groups either in dark or light. The mean iris convexity of the PEX eyes was  $286.3 \pm 63.7 \mu\text{m}$  in the dark and  $251.5 \pm 72.4 \mu\text{m}$  in the light. The mean iris convexity of the fellow eyes was  $239.4 \pm 86.6 \mu\text{m}$  in the dark and  $195.1 \pm 59.3 \mu\text{m}$  in the light. The iris convexity was significantly greater in the PEX eyes than that of their fellow eyes both in the dark and the light ( $P = 0.029$  and  $P = 0.038$ , respectively; paired  $t$ -tests). The convexity of the iris of the fellow eyes was also larger than that of the normal controls but the difference was not significant.

The DMR/SMR ratio in dark for PEX eyes was significantly less than that of the fellow eyes ( $P = 0.037$ ; Tukey-Kramer test). The differences in the DMR/SMR ratio among the three groups in light were not significant (Table 2).

## Iris-Lens Contact Distance (ILCD)

The mean ILCD of PEX eyes was  $0.523 \pm 0.14 \text{ mm}$  in the dark and  $0.908 \pm 0.15 \text{ mm}$  in the light. The mean ILCD of the fellow eyes was  $0.346 \pm 0.12 \text{ mm}$  in the dark and  $0.732 \pm 0.11 \text{ mm}$  in the light. The differences in the ILCD between PEX and fellow eyes were significant both in dark and light ( $P < 0.001$  for both; paired  $t$ -tests; Figure 5). In the light, the ILCD of the fellow eyes was also significantly longer than that of normal control eyes ( $P = 0.035$ ; two-tailed Student's  $t$ -tests; Fig. 5).

## DISCUSSION

Our findings showed that AS-OCT can be used for noninvasive, quantitative, and reliable analyses of the ACA and iris morphol-

ogy in eyes with the PEX syndrome. These findings would probably not be obtained by regular gonioscopy or slit-lamp examination. Analyzing the video files provided us with a useful method to accurately examine the ACA and iris configuration when the pupil was most dilated or constricted. This then allowed us to detect subtle changes between the dark and light conditions.

The differences in the ACA parameters, namely, the AOD500, TISA500, and TIA500, among the three groups were not significant in the dark. However, when the pupil was constricted by light, the PEX eyes had significantly smaller values for all the ACA parameters indicating that the widening of the ACA was significantly more impaired in PEX eyes than in their fellow eyes or normal controls. These findings combined with the smaller ACD in PEX eyes indicate the possibility of a weakness of the zonular fibers and forward shifting of the lens, which is consistent with the previous UBM studies.<sup>10-14</sup> For our PEX patients, although the lens shifting was too small to cause a statistically significant change in the refraction, this alteration could be detected by the highly sensitive AS-OCT analysis.

It is known that melanin granules derived from the iris pigment epithelium and PEX deposits form posterior synechiae starting from the early stages of the PEX process.<sup>1,2</sup> These morphologic changes may account for the poor mydriasis, increased iridolenticular contact, and decreased ability of ACA widening during pupillary constriction.

On the other hand, these morphologic alterations may be pathogenic factors for PEX development or the cause for PEX progression in the PEX process. The morphologic changes may also lead to decreased blood flow or circulatory disturbances resulting in abnormalities in the microenvironment of the anterior chamber such as hypoxia and elevation of cellular stress.<sup>1,2,8</sup> Increased pathologic cytokine or chemokine levels, hypoxic conditions, and circulatory factors in the anterior segment of the eye may also play pivotal roles in the progression of PEX. The relationships among these factors with the morphologic changes need to be investigated.

The iris-lens contact distance (ILCD) was also compared among the three groups. Although ultrasound microscopy can be used for direct measurements of ILCD,<sup>21-23</sup> our study provided a rapid, noncontact method in evaluating this parameter by AS-OCT imaging. The use of Fourier domain AS-OCT provided excellent images of the iris configuration and in combi-

## Comparisons of TIA 500 for PEX, Fellow and Normal Control Eyes

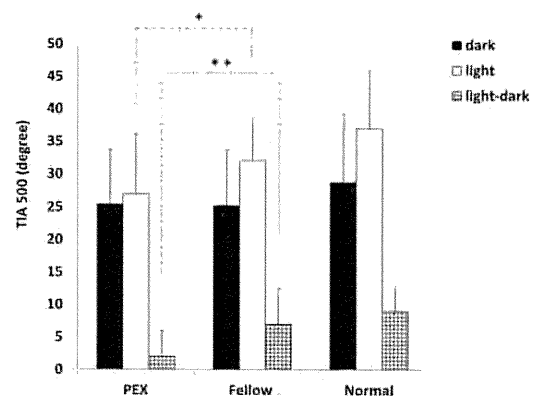


FIGURE 4. Comparisons of TIA500 for eyes with the PEX syndrome, their unaffected fellow eyes, and normal control eyes. Dark, values measured in the dark when pupils were mostly dilated; Light, values measured in the light when pupils were mostly constricted; Light-dark,  $TIA500_{(light)} - TIA500_{(dark)}$ . Statistical significance is denoted by  $**P < 0.01$ , and  $*P < 0.05$ .